Assessment of Magnetic Field Interactions and Radiofrequency-Radiation-Induced Heating of Metallic Spinal Implants in 7 T Field

Itsuko Tsukimura,[1] Hideki Murakami,[1] Makoto Sasaki,[2] Hirooki Endo,[1] Daisuke Yamabe,[1] Ryosuke Oikawa,[1] Minoru Doita[1]

[1]Department of Orthopedic Surgery, School of Medicine, Iwate Medical University, 19-1 Uchimaru, Morioka 020-8505, Japan, [2]Division of Ultrahigh Field MRI, Institute of Biomedical Sciences, Iwate Medical University, Morioka, Japan

Received 17 July 2016; accepted 14 October 2016
Published online 8 March 2017 in Wiley Online Library (wileyonlinelibrary.com). DOI 10.1002/jor.23464

ABSTRACT: The safety of metallic spinal implants in magnetic resonance imaging (MRI) performed using ultrahigh fields has not been established. Hence, we examined whether the displacement forces caused by a static magnetic field and the heating induced by radiofrequency radiation are substantial for spinal implants in a 7 T field. We investigated spinal rods of various lengths and materials, a screw, and a cross-linking bridge in accordance with the American Society for Testing and Materials guidelines. The displacement forces of the metallic implants in static 7 T and 3 T static magnetic fields were measured and compared. The temperature changes of the implants during 15-min-long fast spin-echo and balanced gradient-echo image acquisition sequences were measured in the 7 T field. The deflection angles of the metallic spinal materials in the 7 T field were 5.0–21.0° [median: 6.7°], significantly larger than those in the 3 T field (1.0–6.3° [2.2°]). Among the metallic rods, the cobalt–chrome rods had significantly larger deflection angles (17.8–21.0° [19.8°]) than the pure titanium and titanium alloy rods (5.0–7.7° [6.2°]). The temperature changes of the implants, including the cross-linked rods, were 0.7–1.0°C [0.8°C] and 0.6–1.0°C [0.7°C] during the fast spin-echo and balanced gradient-echo sequences, respectively; these changes were slightly larger than those of the controls (0.4–1.1°C [0.5°C] and 0.3–0.9°C [0.6°C], respectively). All of the metallic spinal implants exhibited small displacement forces and minimal heating, indicating that MRI examinations using 7 T fields may be performed safely on patients with these implants. © 2016 The Authors. *Journal of Orthopaedic Research* Published by Wiley Periodicals, Inc. on behalf of Orthopaedic Research Society. J Orthop Res 35:1831–1837, 2017.

Keywords: 7 T; metallic spinal implants; safety; displacement; heating

Spinal instrumentation surgery using metallic implants, such as rods and screws, is widely performed as an effective treatment for various disorders of the spine and spinal cord, such as scoliosis, spondylosis, fractures, and neoplasms, and was first introduced by Harrington.[1] Patients with spinal metallic implants may be examined using magnetic resonance imaging (MRI). The safety of spinal metallic implants and devices has been thoroughly investigated in MRI performed using magnetic fields of 3 T and less.[2–9] The implants, except for those made from highly ferromagnetic materials, exhibited minimal attraction, and heating by static magnetic fields and radiofrequency (RF) radiation, respectively. In accordance with these results, almost all spinal implants and devices are considered safe or conditionally acceptable in MRI examinations.[10,11]

Recently, ultrahigh-field 7 T MRI has been introduced as a novel imaging process that enables doctors to obtain high-resolution images that are sensitive to susceptibility effects,[12,13] although being still experimental and not completely available for clinical use at this time. For a 7 T magnetic field, the safety of various metallic implants must be revisited because metallic materials can experience unexpectedly strong attractive forces and heating due to the increased static magnetic field strength and RF radiation, respectively. A few reports have been published regarding this issue; however, the studies they described provided no information on spinal metallic implants in 7 T fields.[14–16] Therefore, we investigated whether the displacement forces and heating of various spinal metallic implants are substantial in 7 T fields to ensure the safety of these implants during examinations using ultrahigh-field MRI systems.

MATERIALS AND METHODS

Metallic Spinal Implants

We examined 12 different metallic rods, a screw, and a cross-linking bridge that are frequently used for spinal surgery in clinical practice. The spinal rods were 5.5 mm in diameter; 50, 100, 150, and 200 mm in length; and manufactured from three different types of metals (pure titanium [G869H022], a titanium alloy [G869H021], and cobalt–chrome [1556100500]); while the screw was 6.5 mm in diameter, 58 mm in length, and made of a titanium alloy or cobalt–chrome (55740006540) (CD HORIZON SOLERA Spinal System, Medtronic, Minneapolis, MN). The cross-linking bridge was 8 mm in diameter, 52 mm in length, and composed of a titanium alloy (G811H421) (Low Profile Crosslink Multi-Span Plate, Medtronic, Minneapolis, MN) (Fig. 1). Furthermore, we examined parallel rods (200 mm in length and made of three types of metals) interconnected by two cross-linking bridges, which formed an electrically conductive loop (Fig. 1).

Magnetic-Field-Induced Deflection Test

We examined the interactions between the various metallic spinal implants and the static magnetic fields generated by 7 T and 3 T MRI scanners (Discovery MR950 and MR750,

Grant sponsor: Grant-in-Aid for Strategic Medical Science Research; Grant number: S1491001, 2014–2018; Grant sponsor: Ministry of Education, Culture, Sports, Science, and Technology of Japan.

Correspondence to: Hideki Murakami, (T: +81-19-651-5111; F: +81-19-626-3699; E-mail: hmura@iwate-med.ac.jp)

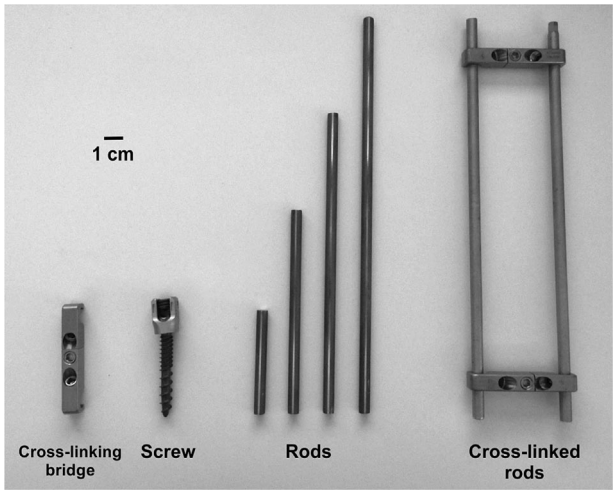

Figure 1. Metallic spinal implants used to examine safety issues in 7 T magnetic field. Magnetic-field-induced displacements and RF-radiation-induced temperature increases were assessed for cross-linking bridge (diameter: 8 mm; length: 52 mm; titanium alloy), screw (diameter: 6.5 mm; length: 57 mm; titanium alloy/cobalt–chrome), rods (diameter: 5.5 mm; length: 50/100/150/200 mm; pure titanium/titanium alloy/cobalt–chrome), and parallel rods interconnected by cross-linking bridges (length: 200 mm; pure titanium/titanium alloy/cobalt–chrome).

respectively, GE Healthcare, Milwaukee, WI) with the maximum spatial gradient of the field strength (dB/dz) of approximately 3.1 T/m (136 cm from the magnet isocenter) and 2.4 T/m (89 cm), respectively, on the axis of the bore.

The deflection angles of the metallic implants in the static magnetic fields were measured using the instrument shown in Figure 2a, in accordance with the deflection angle testing guidelines provided by the American Society for Testing and Materials (ASTM).[16] In each assessment, the material being tested was suspended by a polyester thread (length 4–11 cm [median: 7.25 cm]; weight 0.002–0.003 mg [0.0025 mg]), and the deflection angle of the thread from the vertical line was visually measured using a protractor. These measurements were performed three times when the center of the materials was on the axis of the bore ($x = 0$ cm, $y = 0$ cm) and at positions of 131 cm (7 T) and 85 cm (3 T) from the isocenter of the scanner, at which the deflection angles of metallic materials were the largest in our previous study, indicating the dB/dz is nearly the maximum value on the axis of the bore.[14] The data obtained were then averaged.

RF-Radiation-Induced Heating Test

In accordance to the standard method of measuring RF-radiationinduced heating provided by the ASTM,[17] we measured the temperature changes of the metallic spinal implants during image acquisition by using the 7 T scanner. Each metallic implant was placed on acrylic implant holders in a rectangular polypropylene container ($13 \times 19 \times 26\,cm^3$) filled with a gel saline consisting of 1.32 g/L sodium chloride and 10 g/L polyacrylic acid. Four MRI-compatible fiber-optic thermometer probes with temperature resolutions of 0.1°C and accuracies of 1% full scale (Reflex, Neoptix, Québec, Canada) were placed on the bilateral ends and at the midpoint of each material, as well as 5 cm away from the material to obtain a set of control measurements (CTRL-1) (Fig. 2b). The phantom was left in the scanner room for 6 h or more before the measurements to allow it to achieve equilibrium with the ambient temperature, which was maintained at 19–20°C with a humidity of approximately 50%.

Using the 7 T scanner with quadrature transmission and receiver head coils (size in x, y, and z directions,

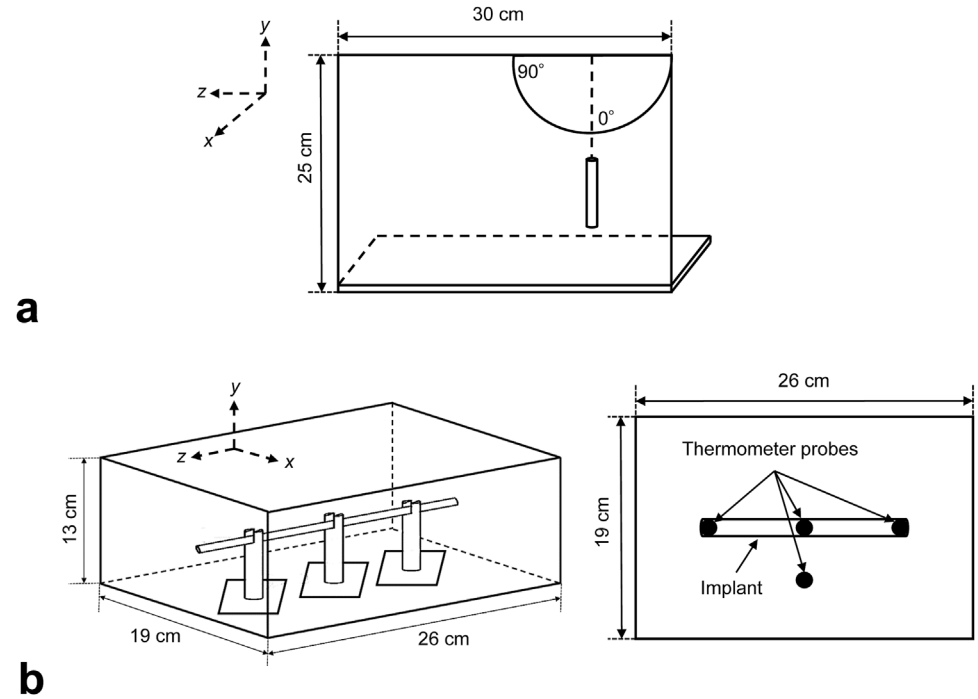

Figure 2. Schematic drawings of devices for measuring magnetic field interactions and RF-radiation-induced heating of metallic spinal implants. (a) Device used to measure deflection angles of materials in 7 T and 3 T static magnetic fields. (b) Phantom and locations of fiber-optic thermometer probes used to measure temperature changes in materials during image acquisition sequences performed using 7 T field.

Table 1. Deflection Angles of Spinal Implants in 3 T and 7 T Fields

Spinal Implant			Averaged Deflection Angle (°)	
Material	Length (cm)	Weight (g)	7 T	3 T
Rod				
Pure titanium	5	5.5	5.0	2.0
	10	10.8	5.8	1.7
	15	16.2	6.2	1.0
	20	21.6	6.2	1.0
	20, cross-linked	66.0	N.A.	N.A.
Titanium alloy	5	5.3	5.7	2.3
	10	10.6	6.5	2.3
	15	15.9	6.8	1.7
	20	21.1	7.7	1.0
	20, cross-linked	65.0	N.A.	N.A.
Cobalt–chrome	5	9.9	17.8	6.0
	10	19.9	19.2	6.3
	15	29.8	20.3	5.7
	20	39.9	21.0	5.0
	20, cross-linked	102.6	N.A.	N.A.
Range (median)	5.0–20.0 (12.5)	5.5–102.6 (19.9)	5.0–21.0 (6.65)	1.0–6.3 (2.15)
Screw				
Titanium alloy/cobalt–chrome	5.8	12.1	10.0	3.2
Cross-linking bridge				
Titanium alloy	5.2	11.4	6.7	2.2

$29 \times 29 \times 28$ cm), image acquisition sequences of longer than 15 min were performed with three-dimensional (3D) fast spin-echo (FSE) and 3D balanced gradient-echo (bGRE) techniques, which are among the imaging techniques that are the most likely to result in RF-radiation-induced heating because of having dense RF duty cycles with large flip angles. The scanning parameters were as follows: For 3D-FSE, repetition time (TR): 740 ms; echo time (TE): 15.5 ms; flip angle (FA): 90–140°; echo train length: 16; bandwidth (BW): 62.5 kHz; and for 3D-bGRE, TR: 8.9 ms; TE: 4.4 ms; FA: 30°; BW: 41.7 kHz. The other parameters, which were used in both techniques, were as follows: Field of view: 256 mm; matrix size: 512×224; slice thickness: 2 mm; number of partitions: 128; number of excitations: 1–2; acquisition time: 15 min (aborted just after the measurements).

The metallic implants were placed within the phantom parallel to the z-axis of the magnet at the center of the transmission head coil and at the center of the static magnetic field ($x = 0$, $y = 0$, $z = 0$). All of the scans were performed using the first-level controlled operating mode, and the intervals between the scans were each at least 10 min in duration. The temperatures of the thermometer probes were recorded in 1 s intervals for 2 min before and 15 min during each image acquisition sequence, and the changes in temperature (Δ°C) from the baseline that was defined as the average temperature during 10 s just before the initiation of the scan were then calculated. The average specific absorption rates (SARs) were also monitored using the scanner console for 6 min during each image acquisition sequence. Furthermore, to obtain another set of control measurements (CTRL-2), the same test was performed at identical probe positions after the implants were removed from the phantoms and the spaces of the implants were filled by the gel.

Statistical Analyses

The differences between the average deflection angles of the implants in the 7 T and 3 T fields were examined using the Wilcoxon signed-rank test, while those of the implants made of different materials and with different lengths were analyzed using the Wilcoxon signed-rank test with Bonferroni correction. To investigate the RF-radiation-induced heating, the largest temperature increases among the three locations on the implants were compared with those in CTRL-1 and CTRL-2 as well as between the imaging techniques and the rods of different materials and lengths by using the Wilcoxon signed-rank test with/without Bonferroni correction. The alpha level used was 0.05.

RESULTS

We successfully performed the magnetic-field-induced deflection and RF-radiation-induced heating measurements for all of the metallic implants.

Magnetic-Field-Induced Deflection Results

The deflection angles of the spinal metallic rods were 5.0–21.0° [median: 6.65°] in the 7 T field and 1.0–6.3° [2.15°] in the 3 T field; the former were significantly greater than the latter ($p = 0.002$, Wilcoxon signed-rank test) (Table 1). Among the materials, the deflection angles of the cobalt–chrome rods (17.8–21.0° [19.7°] in the 7 T field and 5.0–6.3° [5.85°] in the 3 T field) were significantly larger than those of the pure titanium and titanium alloy rods in both fields ($p = 0.035$, Wilcoxon signed-rank test with Bonferroni correction) (Table 1). No significant differences were observed between the rods of different lengths ($p = 0.83$–1.00, Wilcoxon signed-rank test with Bonferroni correction), although

Table 2. Temperature Changes During MRI Sequence(3D-FSE) Performed Using 7 T Field

Spinal Implant			RF-Radiation-Induced Heating (7 T) 3D-FSE (15 min)				
Material	Length (cm)	Weight (g)	Implant (Δ°C)	CTRL-l (Δ°C)	Diff-1 (°C)	CTRL-2 (Δ°C)	Diff-2 (°C)
Rod							
Pure titanium	5	5.5	0.8	0.4	0.4	0.4	0.4
	10	10.8	0.9	1.1	−0.2	0.6	0.3
	15	16.2	0.8	1.0	−0.2	0.8	0
	20	21.6	0.9	0.9	0	0.7	0.2
	20, cross-linked	66.0	1.0	0.9	0.1	0.5	0.5
Titanium alloy	5	5.3	0.7	0.7	0	0.7	0
	10	10.6	0.8	0.9	−0.1	1.1	−0.3
	15	15.9	0.9	0.9	0	0.6	0.3
	20	21.1	0.7	0.9	−0.2	0.7	0
	20, cross-linked	65.0	0.8	0.6	0.2	0.7	0.1
Cobalt–chrome	5	9.9	0.8	0.8	0	0.4	0.4
	10	19.9	0.9	0.3	0.6	0.6	0.3
	15	29.8	0.9	0.3	0.6	0.8	0.1
	20	39.9	0.8	0.5	0.3	0.5	0.3
	20, cross-linked	102.6	0.8	0.6	0.2	0.6	0.2
Range (median)	5–20 (12.5)	5.5–102.6 (19.9)	0.7–1.0 (0.8)	0.3–1.1 (0.8)	−0.2 to 0.6 (0)	0.4–1.1 (0.6)	−0.3 to 0.5 (0.2)
			Screw				
Titanium alloy/ cobalt–chrome	5.8	12.1	0.7	1.0	−0.3	0.5	0.2
Cross-linking bridge							
Titanium alloy	5.2	11.4	0.5	0.7	−0.2	0.5	0

the 20-cm-long rods exhibited the largest deflection angles in the 7 T field (6.2–21.0°). The deflection angles of the screw and the cross-linking bridge were 10.0 and 6.7°, respectively, in the 7 T field and 3.2 and 2.2°, respectively, in the 3 T field.

RF-Radiation-Induced Heating Results

The SAR values during the 3D-FSE and 3D-bGRE acquisition sequences were 2.4–2.8 W/kg [median: 2.5 W/kg] and 2.4–2.6 W/kg [2.5 W/kg], respectively.

During the 15 min 3D-FSE acquisition sequence, the maximum temperature increases of the metallic rods were 0.7–1.0°C [0.8°C], significantly larger than those at the same locations after implant removal (i.e., in CTRL-2), 0.4–1.1°C [0.6°C] ($p = 0.024$, Wilcoxon signed-rank test with Bonferroni correction); however, the temperature increase of 0.3–1.1°C [0.8°C] at the location apart from the implants (i.e., in CTRL-1) was not significantly different ($p = 0.24$, Wilcoxon signed-rank test) (Table 2, Fig. 3). The differences between the temperature increases in the implants and in CTRL-1 and CTRL-2 were −0.2 to 0.6°C [0.0°C] and −0.3 to 0.5°C [0.2°C], respectively (Table 2).

During the 3D-bGRE image acquisition sequences, the temperature increases in the implants were 0.6–1.0°C [0.7°C]; these increases were not significantly different from those of 0.4–0.9°C [0.7°C] and 0.3–0.9°C [0.6°C] in CTRL-1 and CTRL-2, respectively ($p = 0.36$–0.44, Wilcoxon signed-rank test) (Table 3, Fig. 3). There were no significant differences among the rods made of different materials and with different lengths, including the cross-linked rods ($p = 0.18$–1.00, Wilcoxon signed-rank test with Bonferroni correction). Furthermore, the temperature increases in the screw and cross-linking bridge were 0.5–0.7°C [0.65°C], and the differences from the controls were −0.3 to 0.2°C [−0.1°C].

DISCUSSION

In this study, that deflection angles of the spinal implants made from pure titanium or the titanium alloy in the 7 T field were less than 8°. The measurements correspond well with those obtained in previous studies for dental and orthopedic implants made from the same materials.[14,15] These results indicate that the displacement forces on these implants in a 7 T field are minimal compared to gravity, although they are significantly larger than the displacement forces in a 3 T field. Hence, the titanium/titanium alloy implants are considered to be safe in terms of their magnetic field interactions, even in a 7 T field. In contrast, the deflection angles of the cobalt–chrome

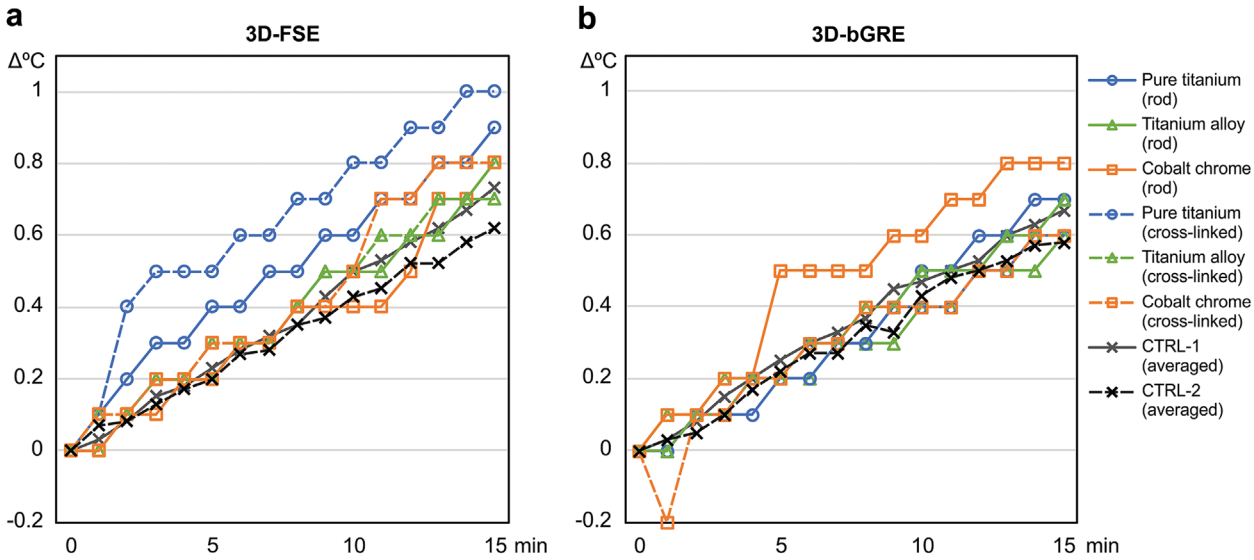

Figure 3. Temperature changes of 200-mm-long metallic spinal rods during image acquisition sequences performed using 7 T field. There are no apparent differences between types of materials or between rods with and without cross-linking. Temperature increases of metallic rods appear similar to those of gel phantom separated from rods (CTRL-1) and those after rod removal (CTRL-2), although temperature increase of rods during 3D-FSE acquisition appear substantial compared to those of CTRL-2. CTRL-1 and CTRl-2 indicate averaged values of the temperature changes with various materials.

spinal rods were 18–21˚, significantly greater than those of the titanium/titanium alloy implants. However, these angles are less than 45˚, which indicates that the deflection force is weaker than gravity, so cobalt–chrome implants are also considered to be safe in 7 T fields according to the ASTM standards.[16]

Regarding RF-radiation-induced heating, the temperature increases in the spinal metallic implants were 1.0˚C or less, even in the worst-case conditions during the 15-min-long, high-SAR image acquisition sequences performed using the 3D-FSE or 3D-bGRE techniques. These results indicate that the RF-radiation-induced heating of spinal implants is negligible because temperature increases of $\leq$1˚C are considered not to induce biological effects in human subjects.[17] In addition, the differences between the temperature increases in the implants and the controls were only 0–0.2˚C, indicating that the heating that resulted from the presence of the metallic implants was minimal even in the 7 T field. Unlike conventional MRI scanners, 7 T scanners lack RF transmission coils for body/spine imaging and only have coils dedicated to head imaging. Hence, many patients' spinal implants cannot receive any RF radiation, provided that the implants are located sufficiently far from the RF transmission coil. Implants in the upper cervical spine may experience RF-radiation-induced heating; however, our results indicate that spinal implants are safe in terms of heating in 7 T fields.

In general, conditions in which electrically closed conductive loops can be formed can cause RF-radiation-induced burn even during acquisition sequences performed within the SAR limits.[18,19] This issue cannot be excluded from spinal implant analysis because cross-linked rods usually form conductive loops. Therefore, in the present study, we examined cross-linked parallel spinal rods that formed conductive loops and were made of three different types of materials, in addition to considering the individual implants. We found that the temperature increase was within 1.0˚C for all of the cross-linked rods and that there were no significant differences from the temperature increases of the individual rods. Hence, cross-linked spinal rods forming conductive loops may be safe in terms of RF-radiation-induced heating in 7 T fields.

This study has several limitations. First, we did not assess the torque exerted on the spinal implants by the static magnetic field. However, spinal implants are always firmly fixed to the spine; thus, there are no substantial torque-related risks, since the implants were minimally deflected by the 7 T field. Second, we did not examine the temperature changes of spinal rods longer than 20 cm because longer rods would have extended beyond the range of the RF transmission head coil. Third, some of the experimental conditions in this study were hardly follow the ASTM guidelines and did not fully cover the worst case scenarios mainly because the size and shape of the materials considerably varied. Thus, our results are considered conditionally limited. In addition, we did not evaluate artifacts induced by the implants on the images, because neither spine nor body coils have been provided for 7 T systems. Furthermore, we did not examine other orthopedic implants and devices, which have been thoroughly investigated in fields of 3 T or less,[4–8,20,21] because these materials were beyond the scope of this study. A previous study showed that certain orthopedic implants, such as femoral/hip joint implants, may involve possible risks.[15] These issues should be investigated in further studies when spine or body

Table 3. Temperature Changes During MRI Sequence(3D-GRE) Performed Using 7 T Field

Spinal Implant			RF-Radiation-Induced Heating (7 T) 3D-bGRE (15 min)				
Material	Length (cm)	Weight (g)	Implant (Δ°C)	CTRL-l (Δ°C)	Diff-1 (°C)	CTRL-2 (Δ°C)	Diff-2 (°C)
Rod							
Pure titanium	5	5.5	0.7	0.4	0.3	0.5	0.2
	10	10.8	0.7	0.8	−0.1	0.5	0.2
	15	16.2	0.6	0.8	−0.2	0.9	−0.3
	20	21.6	0.7	0.7	0	0.8	−0.1
	20, cross-linked	66.0	0.6	0.6	0	0.3	0.3
Titanium alloy	5	5.3	1.0	0.6	0.4	0.5	0.5
	10	10.6	0.7	0.7	0	0.8	−0.1
	15	15.9	0.7	0.7	0	0.6	0.1
	20	21.1	0.6	0.8	−0.2	0.7	−0.1
	20, cross-linked	65.0	0.7	0.6	0.1	0.8	−0.1
Cobalt–chrome	5	9.9	1.0	0.9	0.1	0.5	0.5
	10	19.9	0.7	0.4	0.3	0.8	−0.1
	15	29.8	0.8	0.4	0.4	0.9	−0.1
	20	39.9	0.8	0.5	0.3	0.5	0.3
	20, cross-linked	102.6	0.6	0.8	−0.2	0.4	0.2
Range	5–20	5.5–102.6	0.6–1.0	0.4–0.9	−0.2 to 0.4	0.3–0.9	−0.3 to 0.5
(median)	(12.5)	(19.9)	(0.7)	(0.7)	(0)	(0.6)	(0.1)
Screw							
Titanium alloy/ cobalt–chrome	5.8	12.1	0.7	0.8	−0.1	0.8	−0.1
Cross-linking bridge							
Titanium alloy	5.2	11.4	0.6	0.7	−0.1	0.7	−0.1

CTRL-1, change in temperature 5 cm away from implant; CTRL-2, change in temperature after implant removal; Diff-1, difference of implant from CTRL-1; Diff-2, difference of implant from CTRL-2; Implant, change in temperature of implant.

coils are available. The scanner in this study has not yet approved for the clinical use and is composed of conventional quadrature RF transmit coils and a passive shielding magnet. Future clinically available scanners with novel multichannel transmit coils and active shielding magnet may provide different results from those in this study. Finally, the test method alone appears not sufficient for determining if a device is safe in the clinical MRI environment because the displacement forces and heating effects depend on various factors such as location and direction of materials as well as spatial relationships among materials, human tissues, and transmit coils.

While the present study has various limitations such as those discussed above, it is the first report proving the safety of spinal implants for 7 T MRI in basic experiments. The implants used in spinal surgery are often placed in the vicinity of the spinal cord or cauda equine, and thus represent a type of materials for orthopedic surgery that requires particularly strong evidence for the safety. We believe that this study provides important information for further proving clinical safety of spinal implants and for actual use in clinical settings.

CONCLUSION

Our examinations using a 7 T scanner in accordance with the ASTM guidelines showed that metallic spinal implants, including rods of various lengths and materials, a screw, and a cross-linking bridge, experienced only small displacement forces and minimal heating. The results indicate that MRI examinations using 7 T fields may be performed safely on patients with these implants.

AUTHORS' CONTRIBUTIONS

All the authors contributed to the work described in the paper and all take responsibility for it. Moreover, none of the work described in the paper has been published elsewhere.

ACKNOWLEDGMENT

We are grateful to Tsuyoshi Metoki, RT, for his help with the MRI examinations.

REFERENCES

1. Harrington PR. 1962. Treatment of scoliosis. Correction and internal fixation by spine instrumentation. J Bone Joint Surg Am 44-A:591–610.

2. Rupp R, Ebraheim NA, Savolaine ER, et al. 1993. Magnetic resonance imaging evaluation of the spine with metal implants. General safety and superior imaging with titanium. Spine 18:379–385.
3. Rupp RE, Ebraheim NA, Wong FF. 1996. The value of magnetic resonance imaging of the postoperative spine with titanium implants. J Spinal Dis 9:342–346.
4. Zou YF, Chu B, Wang CB, et al. 2015. Evaluation of MR issues for the latest standard brands of orthopedic metal implants: plates and screws. Eur J Radiol 84:450–457.
5. Shellock FG. 2002. Biomedical implants and devices: assessment of magnetic field interactions with a 3.0-Tesla MR system. J Magn Reson Imaging 16:721–732.
6. Liu Y, Chen J, Shellock FG, et al. 2013. Computational and experimental studies of an orthopedic implant: MRI-related heating at 1.5-T/64-MHz and 3-T/128-MHz. J Magn Reson Imaging 37:491–497.
7. Shellock FG, Audet-Griffin AJ. 2014. Evaluation of magnetic resonance imaging issues for a wirelessly powered lead used for epidural, spinal cord stimulation. Neuromodulation 17: 334–339.
8. Shellock FG, Hatfield M, Simon BJ, et al. 2000. Implantable spinal fusion stimulator: assessment of MR safety and artifacts. J Magn Reson Imaging 12:214–223.
9. McComb C, Allan D, Condon B. 2009. Evaluation of the translational and rotational forces acting on a highly ferromagnetic orthopedic spinal implant in magnetic resonance imaging. J Magn Reson Imaging 29:449–453.
10. Shellock FG. 2015. Reference manual for magnetic resonance safety, implants, and devices. Los Angeles: Biomedical Research Publishing Company.
11. MRIsafty.com. c2016. Playa del Rey: Shellock R & D Services Inc. http://www.mrisafety.com
12. Trattnig S, Bogner W, Gruber S, et al. 2015. Clinical applications at ultrahigh field (7 T). Where does it make the difference? NMR Biomed. [Epub ahead of print].
13. Ugurbil K. 2014. Magnetic resonance imaging at ultrahigh fields. IEEE Trans Biomed Eng 61:1364–1379.
14. Oriso K, Kobayashi T, Sasaki M, et al. 2016. Impact of the static and radiofrequency magnetic fields produced by a 7T MR imager on metallic dental materials. Magn Reson Med Sci 15:26–33.
15. Dula AN, Virostko J, Shellock FG. 2014. Assessment of MRI issues at 7 T for 28 implants and other objects. AJR Am J Roentgenol 202:401–405.
16. American Society for Testing and Materials (ASTM). 2006. ASTM F2052-06 standard test method for measurement of magnetically induced displacement force on passive implants in the magnetic resonance environment. West Conshohocken: ASTM International.
17. American Society for Testing and Materials (ASTM). 2011. ASTM F2182-11a standard test method for measurement of radio frequency induced heating on or near passive implants during magnetic resonance imaging. West Conshohocken: ASTM International.
18. Dempsey MF, Condon B. 2001. Thermal injuries associated with MRI. Clin Radiol 56:457–465.
19. Knopp MV, Essig M, Debus J, et al. 1996. Unusual burns of the lower extremities caused by a closed conducting loop in a patient at MR imaging. Radiology 200:572–575.
20. Muranaka H, Horiguchi T, Usui S, et al. 2006. Evaluation of RF heating on humerus implant in phantoms during 1.5T MR imaging and comparisons with electromagnetic simulation. Magn Reson Med Sci 5:79–88.
21. Yang CW, Liu L, Wang J, et al. 2009. Magnetic resonance imaging of artificial lumbar disks: safety and metal artifacts. Chin Med J 122:911–916.